Conf-911302--17

# EQUILIBRIUM AND NON-EQUILIBRIUM METAL-CERAMIC INTERFACES*

Y. Gao and K. L. Merkle
Materials Science Division
Argonne National Laboratory
Argonne, IL 60439

ANL/CP--74998

DE92 004975

November 1991

The submitted manuscript has been authored by a contractor of the U.S. Government under contract No. W-31-109-ENG-38. Accordingly, the U.S. Government retains a nonexclusive, royalty-free license to publish or reproduce the published form of this contribution, or allow others to do so, for U.S. Government purposes.

* This work was supported by the U. S. Department of Energy, Offices of Basic Energy Sciences - Materials Science under contract #W-31-109-ENG-38.

Manuscript submitted to the 1991 Fall Meeting of the Materials Research Society, Boston, Massachusetts, December 2-6, 1991.

MASTER

# EQUILIBRIUM AND NON-EQUILIBRIUM METAL-CERAMIC INTERFACES

Y. GAO and K. L. MERKLE
Materials Science Division, Argonne National Laboratory, Argonne, IL 60439

## ABSTRACT

Metal-ceramic interfaces in thermodynamic equilibrium ($Au/ZrO_2$) and non-equilibrium (Au/MgO) have been studied by TEM and HREM. In the $Au/ZrO_2$ system, $ZrO_2$ precipitates formed by internal oxidation of a 7%Zr-Au alloy show a cubic $ZrO_2$ phase. It appears that formation of the cubic $ZrO_2$ is facilitated by alignment with the Au matrix. Most of the $ZrO_2$ precipitates have a perfect cube-on-cube orientation relationship with the Au matrix. The large number of interfacial steps observed in a short-time annealing experiment indicate that the precipitates are formed by the ledge growth mechanism. The lowest interfacial energy is indicated by the dominance of closed-packed {111} $Au/ZrO_2$ interfaces. In the Au/MgO system, composite films with small MgO smoke particles embedded in a Au matrix were prepared by a thin film technique. HREM observations show that most of the Au/MgO interfaces have a strong tendency to maintain a dense lattice structure across the interfaces irrespective of whether the interfaces are incoherent or semi-coherent. This indicates that there may be a relatively strong bond between MgO and Au.

## INTRODUCTION

A basic understanding of the structure and composition of metal-ceramic interfaces is of considerable interest because metal-ceramic bonding and adhesion control materials properties in a wide range of applications. It was observed that these interfaces play a dominant role in thin film technology [1], electronic packaging [2], composites [3], ceramic coating and joining [4]. However, information on the structure and composition of these interfaces is still quite limited.

A number of model systems which are not expected to form reaction layers have been studied by several research groups [5-8]. Most of these studies were focused on low-energy interfaces in thermodynamic equilibrium. A common technique to produce these interfaces is internal oxidation of a metallic alloy [5-8] or internal reduction of a doped oxide [8]. It is well established that low-energy interfaces in cubic systems are parallel to the closed-packed {111} lattice planes in both crystals. In most cases, the interfaces incorporate an array of misfit dislocations. However, our understanding of interface structures formed under non-equilibrium conditions is quite embryonic. Studies of such metal-ceramic interfaces is of considerable importance since many systems, especially in technological applications, are far from equilibrium.

In this paper, we describe our initial HREM observations of metal-ceramic interface structures in thermodynamic equilibrium ($Au/ZrO_2$) and non-equilibrium (Au/MgO). In the $Au/ZrO_2$ system, small $ZrO_2$ precipitates in a Au matrix, which were formed by internal oxidation of a 7%Zr-Au alloy, were chosen to study the metal-ceramic interfaces (interface dislocations, steps, and ledges), and the role of the interface ledges in the internal oxidation. In the Au/MgO system, small MgO particles embedded in a Au matrix were chosen to investigate the atomic-scale connection between Au and MgO lattices at the interfaces.

## EXPERIMENTAL

The composite thin films with $ZrO_2$ precipitates in the Au matrix were prepared by electron-beam co-evaporation of Au and Zr. The Au-Zr alloy films with an average thickness of 100 nm for Au and 7 nm for Zr were simultaneously deposited on (100) cleaved and (110) polished surfaces

EB

of NaCl substrates at 325 °C. Deposition rates of Au and Zr were 0.2 to 0.3 nm/s and 0.01 to 0.02 nm/s, respectively. The composite films were then annealed on their substrates in vacuum at 325 °C for 30 min. The composite films were separated from the NaCl substrates in water and picked up on Au microscopic grids. Subsequently, alloy films were internally oxidized in a 0.2% $O_2$/Ar atmosphere at 600 °C for 2 hrs and for 14 hrs, respectively.

The composite thin films with the MgO smoke particles in the Au matrix were prepared by collecting MgO smoke particles onto NaCl substrates, followed by vacuum deposition of Au. By burning a thin Mg wire in air, MgO smoke particles were obtained and collected on (110) NaCl substrates. Subsequently, Au was deposited in vacuum on the substrates held at 300 °C. On their substrates the films (~80 nm thick) were annealed in Ar at 350 °C for 1 hr to form good joints between the MgO particles and the Au matrix. The films were then separated from the substrates in water and mounted on Au grids. The final specimens for electron microscopy observations were prepared by argon ion-beam thinning. In this manner thin areas were obtained with thickness less than 10 nm. A liquid-nitrogen-cooled stage was used during ion thinning. All HREM images were obtained at close to axial illumination for several defocus values near the optimum focus condition.

## RESULTS AND DISCUSSION

### Equilibrium Interfaces

A typical microstructure of the Au/$ZrO_2$ composite films annealed for 2 hrs is shown in Fig. 1a, where the small precipitates are $ZrO_2$. The size of the $ZrO_2$ precipitates varies from 1 nm to 5 nm, and their shape is irregular. Selected-area electron diffraction patterns in Fig. 1b from a (100) film and in Fig. 1c from a (110) film indicate that the $ZrO_2$ phase is cubic and most of the precipitates have a perfect cube-on-cube orientation relationship with the Au matrix. It is known that cubic $ZrO_2$ is stable only at high temperature above 1400 °C [9]. However, the cubic phase can be preserved by quenching to room temperature if some impurity such as MgO is present [9]. In the present study, high purity materials were used, e.g. 99.9999% Au and 99.95% Zr. Hence, it is unlikely that formation of the cubic phase was due to impurity contamination. Since the $ZrO_2$ precipitates were nucleated and grown within the Au matrix, the structure of the $ZrO_2$ phase was restrained by the matrix, which must have acted as a template for the nucleation of $ZrO_2$. Consequently, the $ZrO_2$ precipitates slightly deviated from the stable structure at that temperature, and formed the cubic phase. Furthermore, the lattice parameter measured from the diffraction patterns (0.509 nm) and from HREM images (0.508 nm) matches the lattice parameter (0.507 nm) of the cubic phase quite well [9].

A HREM image of a small $ZrO_2$ precipitate in the Au matrix is shown in Fig. 2. The Au/$ZrO_2$ interfaces appear sharp with no evidence of existence of an intermediate layer or a second phase. Furthermore, it is clearly seen that the small particle is strongly faceted on an atomic scale

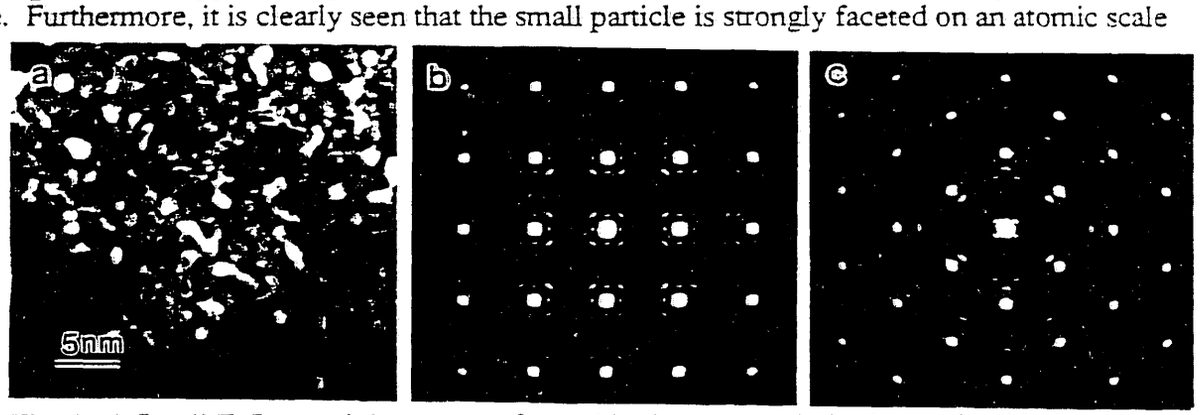


Fig. 1 a) Small $ZrO_2$ precipitates were formed in the Au matrix by internal oxidation of a 7%Zr-Au alloy. Selected-area electron diffraction patterns in b) from a (100) film and in c) from a (110) film indicate that the $ZrO_2$ phase is cubic and most of the precpitates have a cube-on-cube orientation relationship with the Au matrix.

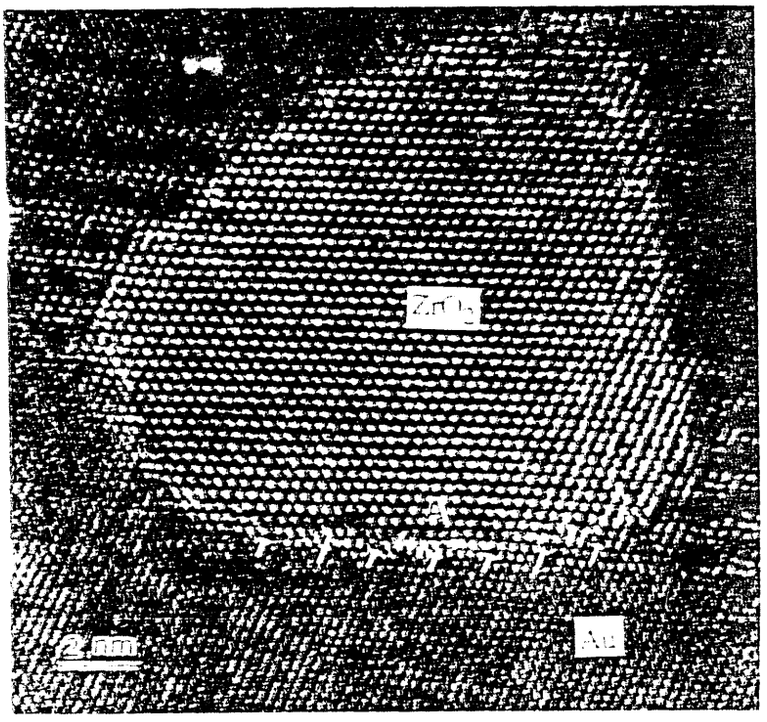
ZnO
Au
2 nm

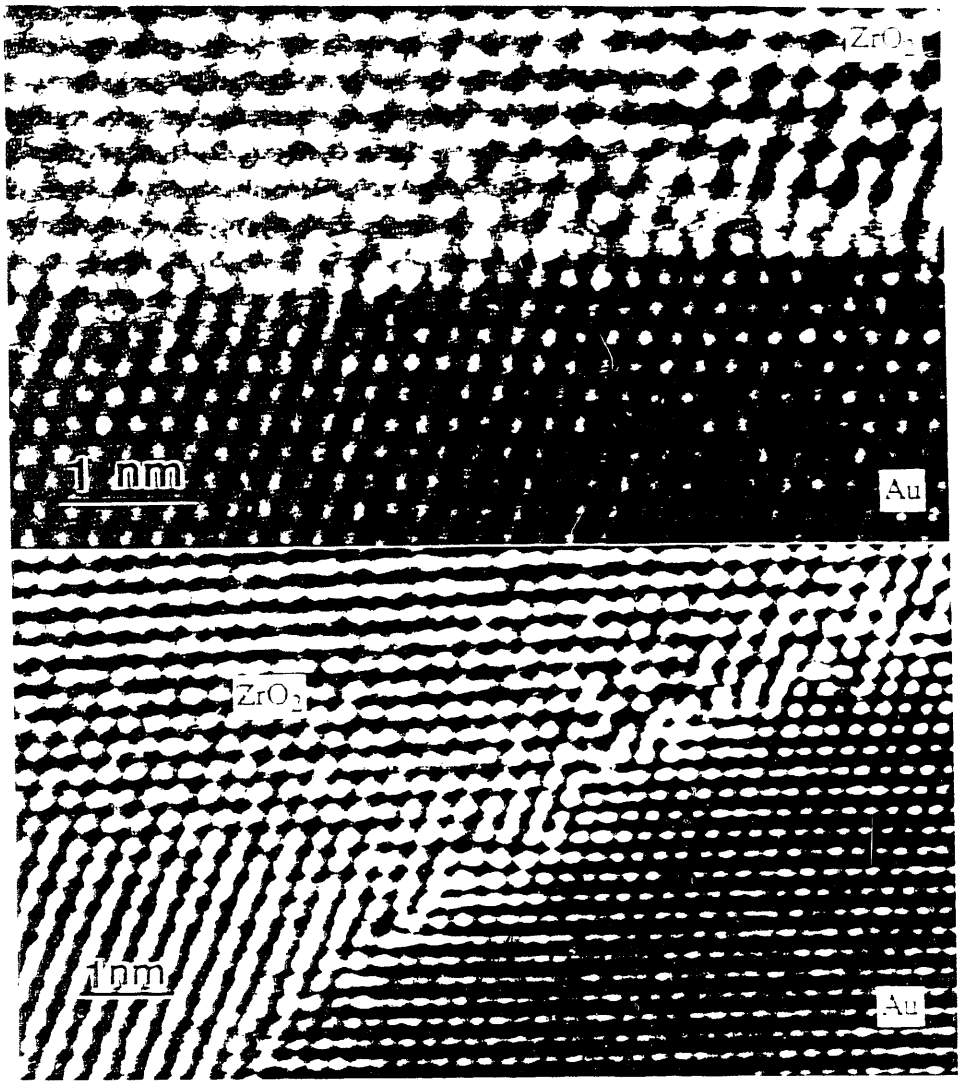


Fig. 3 a) HREM image of a {111} Au/$ZrO_2$ interface, incorporating an array of misfit dislocations; b) Interfacial steps observed at a $ZrO_2$ precipitate edge

the ($\bar{1}$11) Au lattice planes across the interface, resulting in a quite large misfit (11%). It can be seen that nine (020)MgO fringes match very well with eight ($\bar{1}$11) Au fringes at this interface. Misfit dislocations with localized core structures can be observed, as indicated by T.

Another well-connected interface is shown in Fig. 4b, where the (200)MgO planes are parallel to the interface and the (002)Au planes are inclined to the interface by about 5°. The interface appears atomically flat, and the (020)MgO lattice planes connect with the ($\bar{1}$11)Au planes at an angle of about 30°. Thus, the misfit between the MgO lattice fringes and the projections of the ($\bar{1}$11)Au lattice fringes is ~ 25% at the interface, resulting in a (020) terminating fringe in every four (020)MgO lattice fringes. These terminating fringes can be observed in Fig. 4b, as indicated by arrows. No evidence for coherence is found, therefore this interface must be incoherent. However, the interface is very dense without any large open area, and the Au/MgO joining also appears very good. This has been found to be true for all Au/MgO interfaces observed no matter whether the interfaces are incoherent or semi-coherent.

In some cases, however, a quite large number of steps can be observed at the Au/MgO interfaces. An example of such an interface is shown in Fig. 4c. The step height corresponds to the spacing of the {111}Au lattice planes. The formation of these monolayer steps is likely to accommodate the small misorientation (~7°) between the (200)MgO and ($\bar{1}$11)Au lattice planes, and thus to reduce the lattice mismatch across the interface. Furthermore, the formation of these steps indicates that a strong reconstruction or relaxation could occur at the interface since the MgO smoke particles are rectangular with large flat {100} faces. This also suggests that {200}MgO/{111}Au interfaces are low-energy interfaces. The {200}/{111} interfaces have been found to be low-

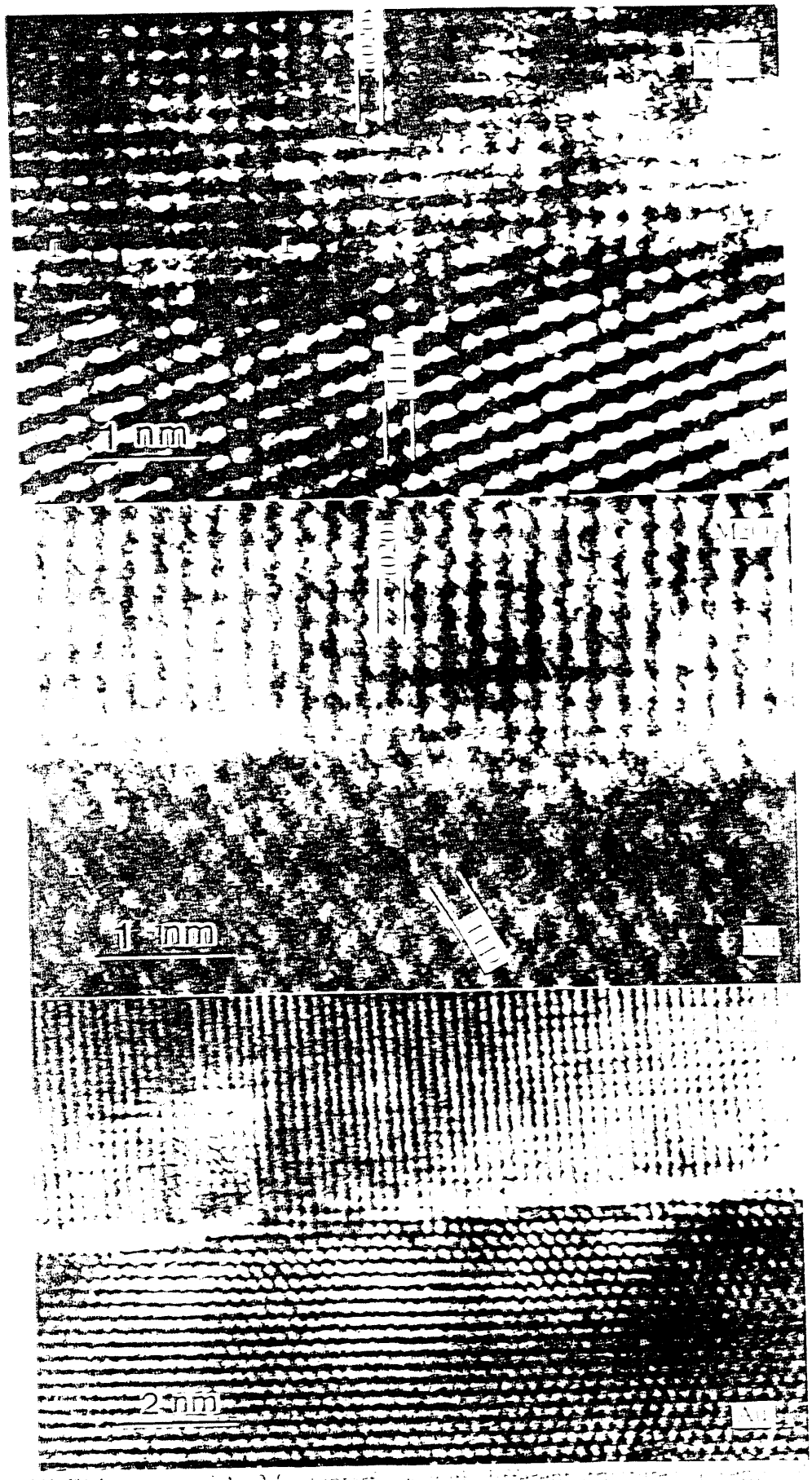
1 nm
1 nm
2 nm

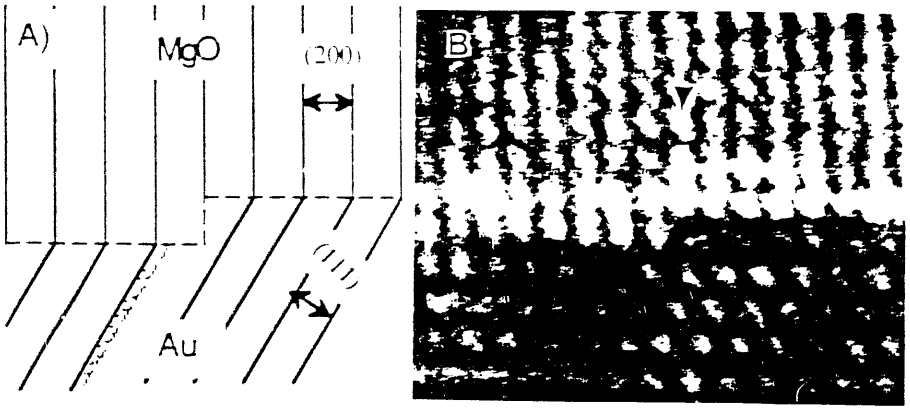


Fig. 5 a) Interfacial step corresponding to a misfit dislocation; b) HREM image of such a step.

energy interfaces in the Ag/Ni system [11]. The interfacial steps of height $d_{(111)Au}$ can correspond to misfit dislocations at the interface, as depicted in Fig. 5a. The shaded areas represent the atomic displacement of (111) Au lattice planes. This kind of misfit dislocation can be observed in Fig. 4c. An enlarged image of such a dislocation is shown in Fig. 5b. Clearly, the misfit at the interface is accommodated both by the interfacial steps and the misfit dislocations, resulting in an atomically well-connected interface.

## CONCLUSIONS

The present study of the $ZrO_2$ precipitates in the Au matrix formed by internal oxidation of a 7%Zr-Au alloy shows that the $ZrO_2$ precipitate phase is cubic. Formation of cubic $ZrO_2$ is likely to originate as a template effect of the Au matrix. Most of the $ZrO_2$ precipitates have a perfect cube-on-cube orientation relationship with the Au matrix. A large number of interfacial steps observed in the short-time annealing experiment indicate a ledge growth mechanism. The closed-packed {111} Au/$ZrO_2$ interfaces appear to have the lowest interfacial energy. These interfaces are semi-coherent, and the large misfit (22%) is accommodated by misfit dislocations. In the Au/MgO system, HREM images of a number of the Au/MgO interfaces with different misorientations and structures show that most of the interfaces have a strong tendency to maintain a dense lattice structure across the interfaces irrespective of whether the interfaces are incoherent or semi-coherent. This indicates that there may be relatively strong bonding between MgO and Au.

## ACKNOWLEDGEMENTS

This work was supported by the U. S. Department of Energy, Basic Energy Sciences - Materials Science under contract No. W-31-109-ENG-38. The use of the H-9000 in the Dept. of Mater. Sci. & Eng., Northwestern University is gratefully acknowledged.

## REFERENCES

1. B. W. Dodson, L. J. Schowalter, J. E. Cunningham, F. H. Pollak (eds.), Layered Structures - Heteroepitaxy, Superlattices, Strain, and Metastability, MRS Symp. Proc. Vol. 160.
2. E. D. Lillie, P. S. Ho, R. Jaccodine, K. Jackson (eds.), Electronic Packaging Materials Science V, MRS Symp. Proc. Vol. 203 (Materials Research Society, Pittsburgh, 1991).
3. R. Y. Lin, R. J. Arsenault, G. P. Martins, S. G. Fishman (eds.), Interfaces in Metal-Ceramics Composites, TMS Proc. (The Minerals, Metals & Materials Society, 1990).
4. M. M. Schwartz, *Ceramic Joining*, ASM International (Materials Park, Ohio, 1990).
5. W. Mader, Mater. Res. Symp. Proc. **82**, 403 (1987).
6. G. Necker and W. Mader, Phil. Mag. Lett. **58**, 205 (1988).
7. F. Ernst, P. Pirouz, A. H. Heuer, MRS Symp. Proc. **103**, 557 (1989).
8. K. L. Merkle, in Metal-Ceramic Interfaces, ed. by M. Ruhle, A. G. Evans, M. F. Ashby, J. P. Hirth, Pergamon Press (1990) p. 242.
9. R. W. G. Wyckoff, Crystal Structures, 2nd Edition, Vol. 1, Interscience Publishers (1963).
10. J. P. Hirth, Metall. Trans. A, **22**, 1331 (1991).
11. Y. Gao, P. G. Shewmon, S. A. Dregia, Acta Metall. **37**, 3165 (1989).

# END

DATE
FILMED
02/11/92